BIOCHEMISTRY
including biophysical chemistry & molecular biology
Article

Biochemistry **2009,** *48,* 10905–10917 10905
DOI: 10.1021/bi9009874

Design of Nontoxic Analogues of Cathelicidin-Derived Bovine Antimicrobial Peptide BMAP-27: The Role of Leucine as Well as Phenylalanine Zipper Sequences in Determining Its Toxicity[†]

Aqeel Ahmad,[‡] Sarfuddin Azmi,[‡,∥] Raghvendra M. Srivastava,[‡,∥] Saurabh Srivastava,[‡] Brijesh K. Pandey,[‡] Rubha Saxena,[‡] Virendra Kumar Bajpai,[§] and Jimut Kanti Ghosh*[,‡]

[‡]*Molecular and Structural Biology Division and* [§]*Electron Microscopy Unit, Central Drug Research Institute, CSIR, Lucknow 226001, India.* [∥]*These authors contributed equally to this work.*

Received June 12, 2009; Revised Manuscript Received October 7, 2009

ABSTRACT: BMAP-27 is a cathelicidin-derived bovine antimicrobial peptide, which shows moderate cytotoxicity and potent antibacterial activity against a wide variety of microorganisms. Despite a number of studies, very little is known about the amino acid sequences of this peptide that controls its antibacterial and cytotoxic activities. Small stretches of phenylalanine and leucine zipper sequences were identified at the N- and C-termini of the molecule, respectively. To understand the structural and functional roles of these sequence elements, we synthesized and characterized several analogues of BMAP-27 after substituting leucine or phenylalanine residue(s) at **a** and/or **d** positions of the leucine and phenylalanine zipper sequences, respectively, with alanine. BMAP-27 analogues exhibited significantly reduced cytotoxicity against the human red blood (hRBC) and murine 3T3 cells as compared to that of the wild-type peptide. Interestingly, BMAP-27 and its analogues exhibited comparable antibacterial activity against the selected Gram-positive and Gram-negative bacteria. Moreover, BMAP-27 and its analogues exhibited similar localization and assembly onto the selected bacteria and induced comparable permeability in these cells. However, only BMAP-27, not its analogues, assembled and bound strongly onto the hRBCs and permeabilized them. The results indicated that not only a leucine zipper but also a phenylalanine zipper sequence plays an important role in maintaining the assembly of BMAP-27 on the mammalian cells examined here and cytotoxic activity against them. To the best of our knowledge, this is the first report of the evaluation of structural and functional roles of a phenylalanine zipper sequence in a naturally occurring antimicrobial peptide.

Cationic antimicrobial peptides are an integral part of the host immune system, which constitutes cathelicidins, defensins, and other families of peptides (*1*−*8*). The term cathelicidin was introduced to encompass bipartite molecules containing a cathelin domain and a C-terminal antimicrobial peptide domain (*2*, *4*−*6*, *8*). Cathelin was first isolated as a 96-residue porcine peptide. The cathelicidin family shares considerable amino acid sequence homology with the cathepsin family of cysteine protease inhibitors.

Cathelicidin-derived peptides have a diverse range of activity against Gram-negative and Gram-positive bacteria, parasites, and enveloped viruses (*9*−*13*). Besides activities against different microorganisms, these peptides also exhibit other important biological activities that include wound healing, inhibition of tissue injury, angiogenesis, repair of skin disorder, etc. (*14*−*17*).

To date, cathelicidin-derived antimicrobial peptides have been described in a wide variety of vertebrates, including humans (*18*−*20*), cattle, fish, birds, etc. (*4*, *13*, *21*). Recent studies on human cathelicidin-derived antimicrobial peptide LL-37 and its primate orthologues revealed interesting data (*22*, *23*). Macaque and leaf-eating monkey RL-37 peptides contained more positive charges like other helical antimicrobial peptides found in insects and frogs, were monomeric and unstructured in bulk solution, and had a potent, salt- and medium-independent antimicrobial activity in vitro (*22*). In contrast, human LL-37 is less cationic and exhibited a salt-dependent structuring and aggregation that influenced its antimicrobial activity and mode of action (*22*, *23*). The structurally diverse cathelicidin-derived antimicrobial peptides of animals provide interesting and potential models for pharmaceutical development. Several properties of the cathelicidin-derived peptides make them attractive candidates for research and drug development (*24*). They are effective killers of many microorganisms. More advantageous is their retaining bactericidal activity even at a physiological or elevated salt concentration. Their synthesis is economically viable because of the absence of disulfide bridges. Moreover, their speedy rate of killing is an added benefit in topical usage.

BMAP-27, an antimicrobial peptide of bovine origin, also exhibits a potent and broad-spectrum antibacterial activity and is also cytotoxic to human erythrocytes and neutrophils (*25*). The cytotoxic property of these peptides is an indication of their poor discrimination between the prokaryotic and eukaryotic membranes. Effort has been made to increase the selectivity of these molecules toward the microbes. BMAP-27(1−18) was virtually

[†]The work was supported by CSIR Network Project NWP 0005. A.A., S.A., and B.K.P. acknowledge the receipt of a senior research fellowship from CSIR, India, and S.S. acknowledges a junior research fellowship from CSIR, India.

*To whom correspondence should be addressed. Telephone: 091-522-2612411-18, ext. 4282. Fax: 091-522-2623405. E-mail: jighosh@yahoo.com.

© 2009 American Chemical Society
Published on Web 10/21/2009

devoid of cytotoxic activities and displayed an antimicrobial potency slightly lower than that of the parent molecule (*25*). The structure−function correlation studies implied that the hydrophobic C-terminal tail is the major determinant of the cytotoxicity of the BMAP molecule toward mammalian cells (*25*).

Recently, we identified and characterized an amphipathic leucine zipper motif in melittin (*26*). Substitution of heptadic leucine(s) with one or two alanine residues appreciably reduced the cytotoxic activity of melittin without significantly affecting its antibacterial activity. Moreover, novel antibacterial peptides were designed on the basis of a classical amphipathic leucine zipper sequence with or without alanine substitution at the **a** and/or **d** position of the heptad repeat, which showed remarkable variation in hemolytic activity against human red blood cells but exhibited almost similar antibacterial activity (*27*). However, it is still not clear whether the leucine zipper or the heptad repeat sequences possess any role in controlling the cytotoxicity in other naturally occurring antimicrobial peptides. Toward this end, a long heptad repeat sequence was identified in bovine antimicrobial peptide BMAP-27. The C-terminus of the sequence contains a small leucine zipper sequence and the N-terminus a phenylalanine zipper sequence. Several alanine-substituted analogues of BMAP-27 were designed for the investigation of the role of these phenylalanine and leucine zipper sequences.

The mechanism of killing of prokaryotic and eukaryotic cells by BMAP-27 is not clear, although it is believed that the peptide-induced membrane permeabilization of a target cell could be the key step behind it. To understand the mode of action of BMAP-27 and its novel analogues, we directly assessed the peptide-induced depolarization and integrity of bacterial and mammalian cell membranes. Also, the localization and assembly of BMAP-27 and its analogues onto bacterial and human red blood cells were studied to understand the basis of their cytotoxic and antibacterial activities against the mammalian cells and bacteria.

MATERIALS AND METHODS

Materials. Rink amide MBHA resin (loading capacity, 0.63 mmol/g) and all the N-α Fmoc- and side chain-protected amino acids were purchased from Novabiochem. Coupling reagents for peptide synthesis like 1-hydroxybenzotriazole, *N*,*N*′-diisopropylcarbodiimide (DIC), 1,1,3,3-tetramethyluronium tetrafluoroborate, and *N*,*N*′-diisopropylethylamine were purchased from Sigma, while dichloromethane, *N*,*N*′-dimethylformamide, and piperidine were of standard grades and procured from reputed local companies. Acetonitrile (HPLC grade) was procured from Merck, whereas trifluoroacetic acid (TFA) was purchased from Sigma. Egg phosphatidylcholine (PC)[1] and egg phosphatidylglycerol (PG) were procured from Northern Lipids Inc. (Burnaby, BC), while cholesterol (Chol) was purchased from Sigma. 3,3′-Dipropylthiadicarbocyanine iodide (diS-C_3-5) and NBD (4-fluoro-7-nitrobenz-2-oxa-1,3-diazole) fluoride were purchased from Invitrogen (Molecular Probes, Eugene, OR). The rest of the reagents were of analytical grade and procured locally; buffers were prepared in milli Q (USF^{ELGA}) water.

Peptide Synthesis, Fluorescent Labeling, and Purification. Stepwise solid phase syntheses of all the peptides were conducted manually on rink amide MBHA resin (0.15 mmol) utilizing the standard Fmoc chemistry, reported previously (*28*, *29*). Labeling at the N-terminus of peptides with a fluorescent probe, cleavage of the labeled and unlabeled peptides from the resin, and their precipitation and purification by reverse phase HPLC were achieved by standard procedures (*26*, *29*). The purified peptides were ∼95% homogeneous. Experimental molecular masses of the peptides, detected by MALDI-TOF or ESI-MS analysis, corresponded closely with the desired values.

Assay of Antibacterial Activity of the Peptides. The antibacterial activity of the peptides was assayed in a sterile 96-well plate in a final volume of 100 μL under aerobic conditions (*26*, *30*, *31*). In brief, a 50 μL bacterial culture, grown in LB medium with 10^6 CFU/mL, was added to 50 μL of water containing different peptides serially diluted 2-fold in each well and incubated for 18−20 h at 37 °C. The peptides' antibacterial activities, expressed as their MICs (the peptide concentration that results in 100% inhibition of microbial growth), were assessed by measuring the absorbance at 492 nm. The microorganisms used were Gram-positive bacteria, *Bacillus subtilis* ATCC 6633 and *Staphylococcus aureus* ATCC 9144, and Gram-negative bacteria, *Escherichia coli* ATCC 10536 and DH5α.

The bactericidal activity of BMAP-27 and its analogues was tested against *E. coli* ATCC 10536 and *B. subtilis* ATCC 6633 in the presence of heat-inactivated serum as described by others (*32*), except FBS was used instead of human serum. The final concentration of serum in the antibacterial activity assay medium was 25% (v/v).

Hemolytic Activity Assay. The hemolytic activity of these designed peptides was assayed against fresh hRBCs that were collected in the presence of an anticoagulant from a healthy volunteer and washed three or four times by PBS by a standard procedure (*26*, *27*, *30*). Peptides, dissolved in water, were added to the suspension of red blood cells [final concentration of 6% (v/v)] in PBS until a final volume of 200 μL was reached and incubated at 37 °C for 30 min. The samples were then centrifuged for 10 min at 2000 rpm, and the release of hemoglobin was monitored by measuring the absorbance (A_{sample}) of the supernatant at 540 nm. For negative and positive controls, hRBCs in PBS (A_{blank}) and in 0.2% (v/v, final concentration) Triton X-100 (A_{triton}) were used, respectively. The percentage of hemolysis was calculated according to the following equation (*26*, *30*).

$$\text{percentage of hemolysis} = [(A_{sample} - A_{blank})/(A_{triton} - A_{blank})] \times 100$$

MTT Assay. The MTT [3-(4,5-dimethylthiazol-2-yl)-2,5-diphenyltetrazolium bromide] assay was performed to check the toxic activity of peptides against murine 3T3 cells by a standard procedure as reported previously (*33*); 10000 cells per well were seeded in 96-well plates, and overnight incubation was conducted in a CO_2 incubator for adherence. The complete media were discarded from the plate, and incomplete media were added. After that, different concentrations of peptides were added and the plates incubated for 2 h. Then 10 μL of MTT (5 mg/mL) solutions was added to each well, and the plates were again incubated for 2 h. Incomplete media were discarded from 96-well plates, and 200 μL of DMSO was added to each well to dissolve

[1]Abbreviations: hRBCs, human red blood cells; Fmoc, *N*-(9-fluorenyl)methoxycarbonyl; Chol, cholesterol; HPLC, high-performance liquid chromatography; CFU, colony-forming unit; PC, egg phosphatidylcholine; PG, egg phosphatidylglycerol; NBD, 4-fluoro-7-nitrobenz-2-oxa-1,3-diazole; MALDI-TOF, matrix-assisted laser desorption ionization time-of-flight; PBS, phosphate-buffered saline; MICs, minimum inhibitory concentrations; MTT, 3-(4,5-dimethylthiazol-2-yl)-2,5-diphenyltetrazolium bromide; FRET, fluorescence resonance energy transfer; ANS, 1-anilino-8-naphthalene sulfonate.

the crystal. The well to which no peptide was added was considered the control. Reading of these samples was recorded at 550 nm by a microplate reader.

Analysis of Peptide-Induced Membrane Damage of 3T3 and E. coli Cells by Flow Cytometry. Peptide-induced membrane damage of 3T3 cells was assessed by staining the cells with propidium iodide after the treatment with the peptides at 37 °C for 15 min. These cells were then analyzed by flow cytometry in the form of a dots plot with respect to the control cells, not treated with any peptide. To check the membrane integrity of bacteria after peptide treatment, the cells (*E. coli* DH5α or *E. coli* ATCC 10536) at midlog phase were incubated with BMAP-27 and its alanine-substituted analogues for 30 min at 37 °C with constant shaking. The cells were collected by centrifugation, washed two times with PBS, and incubated further with propidium iodide at 4 °C for 30 min, followed by removal of the unbound probe through washing with an excess of PBS and resuspension in buffer. Peptide-induced damage of bacterial cells was then analyzed by flow cytometry.

Assay of the Peptide-Induced Depolarization of hRBCs and an E. coli Cell Membrane. Peptide-induced depolarization of hRBCs and an *E. coli* DH5α (mentioned as *E. coli* throughout the text unless stated otherwise) membrane was detected by its efficacy to dissipate the potential across these cell membranes (*34*, *35*). Fresh human red blood cells (hRBCs) were collected in the presence of an anticoagulant from a healthy volunteer, washed three times in PBS, and resuspended in the same buffer with a final cell density of $\sim 3.0 \times 10^7$ cells/mL. Human red blood cells were incubated with a diS-C_3-5 probe for 1 h. When the fluorescence level (excitation and emission wavelengths set at 620 and 670 nm, respectively) of the hRBCs became stable, different amounts of each of the peptides were added to these suspensions and incubated at 37 °C for 30 min. After that, peptide-induced membrane depolarization of human red blood cells was recorded. The bacteria were grown at 37 °C until they reached midlog phase, centrifuged, and washed with buffer [20 mM glucose and 5 mM HEPES (pH 7.3)]. Then bacteria were resuspended (final concentration of $\sim 2 \times 10^5$ CFU/mL) in a similar buffer containing 0.1 M KCl and incubated with a diS-C_3-5 probe for 1 h. When the fluorescence level of the bacterial suspension became stable, different amounts of each of the peptides were added to these suspensions to record the peptide-induced membrane depolarization of the bacterial membrane. Membrane depolarization as measured by the fluorescence recovery (F_t) was defined by the equation (*29*, *36*, *37*) $F_t = [(I_t - I_0)/(I_f - I_0)] \times 100\%$, where I_f, the total fluorescence, was the fluorescence levels of cell suspensions just after addition of diS-C_3-5; I_t is the observed fluorescence after the addition of a peptide at a particular concentration either to hRBCs or to *E. coli* suspensions, which were already incubated with diS-C_3-5 probe for 1 h; and I_0 is the steady fluorescence level of the cell suspensions after incubation with the probe for 1 h. Fluorescence was monitored at 670 nm with respect to time (seconds) with an excitation wavelength of 620 nm. Excitation and emission slits were set at 8 and 6 nm, respectively.

Assay of Peptide-Induced Depolarization of Zwitterionic and Negatively Charged Lipid Vesicles. The ability of the peptides to destabilize the phospholipid bilayer was detected by their efficacy to dissipate the diffusion potential across the membrane. For this purpose, both zwitterionic PC/Chol (8:1, w/w) and negatively charged PC/PG (1:1 w/w) (*38*−*40*) lipid vesicles were prepared in K^+ buffer [50 mM K_2SO_4 and 25 mM HEPES-sulfate (pH 6.8)]. Required amounts of the lipid vesicles were mixed with isotonic (K^+-free) Na^+ buffer [50 mM Na_2SO_4 and 25 mM HEPES-sulfate (pH 6.8)] followed by the addition of the potential sensitive dye diS-C_3-5. Addition of valinomycin created a negative potential inside the lipid vesicles by the selective efflux of K^+ ions from the lipid vesicles. As a result of that, a quenching of the fluorescence of the dye occurred. When the dye exhibited a steady fluorescence level in the presence of lipid vesicles, peptides were added. Membrane permeability of the peptide was detected by the increase in fluorescence, which resulted from the dissipation of diffusion potential. The peptide-induced dissipation of diffusion potential was measured in terms of the percentage of fluorescence recovery (F_t) by the same equation as shown in the previous section. Here, I_t is the observed fluorescence after the addition of a peptide at time t (~5 min after the addition of the peptide), I_0 is the fluorescence after the addition of valinomycin, and I_f is the total fluorescence observed before the addition of valinomycin. Excitation and emission wavelengths of diS-C_3-5 and excitation and emission slits were the same as those described above.

Detection of Release of Calcein from the Calcein-Entrapped Lipid Vesicles. Peptide-induced calcein release from calcein-entrapped lipid vesicles has often been employed in the detection of the pore forming activity of proteins and peptides. Calcein-entrapped lipid vesicles were prepared with a self-quenching concentration (60 mM) of the dye in 10 mM HEPES (pH 7.4) as reported previously (*29*, *41*). Briefly, a thin film of lipid (PC/PG or PC/Chol) was resuspended in a calcein solution, vortexed for 1−2 min, and then sonicated in a bath-type sonicator. The nonencapsulated calcein was removed from the liposome suspension by gel filtration using a Sephadex G-50 column. Usually, lipid vesicles become approximately 10-fold diluted after passing through a G-50 column. The eluted calcein-entrapped vesicles were further diluted in the same buffer to a final lipid concentration of ~3.0 μM for the experiment. Peptide-induced release of calcein from the lipid vesicles was detected by an increase in fluorescence due to the dilution of the dye from its self-quenched concentration. Fluorescence was monitored at room temperature with excitation and emission wavelengths fixed at 490 and 520 nm, respectively. Calcein release as measured by the fluorescence recovery is defined by the same equation that was used to determine the peptide-induced depolarization of hRBCs and bacteria or the dissipation of diffusion potential in lipid vesicles in the previous sections. However, in this case, I_f, the total fluorescence, was determined after the addition of Triton X-100 (final concentration of 0.1%) to the dye-entrapped vesicle suspension. Excitation and emission slits were fixed at 8 and 6 nm, respectively.

Circular Dichroism Experiments. CD spectra of the peptides were recorded in PBS, and in the presence of 40% (v/v) TFE (in water) and 1% (v/v) SDS (in water) by utilizing a Jasco J-810 spectropolarimeter. The samples were scanned at room temperature (~30 °C) in a capped quartz cuvette with a path length of 0.20 cm in the wavelength range of 250−195 nm. The fractional helicities were calculated with the help of mean residue ellipticity values at 222 nm by the following equation (*42*, *43*).

$$F_h = \frac{[\theta]_{222} - [\theta]^0_{222}}{[\theta]^{100}_{222} - [\theta]^0_{222}}$$

where $[\theta]_{222}$ is the experimentally observed mean residue ellipticity at 222 nm. The values for $[\theta]^{100}_{222}$ and $[\theta]^0_{222}$ that

correspond to 100 and 0% helix contents were considered to have mean residue ellipticity values of −32000 and −2000, respectively, at 222 nm.

Detection of Binding of ANS to Peptides. ANS (~20 μM) fluorescence was recorded in the presence of each of the peptides at a concentration of ~47.0 μM. The excitation wavelength and emission wavelength range for ANS were set at 365 and 410−600 nm, respectively (*44*). The excitation and emission slits were fixed at 6 and 4 nm, respectively.

Confocal Microscopy Experiments. Localization and binding of the peptides onto the hRBCs and *E. coli* DH5α were assessed with the help of their Rho-labeled analogues by employing a Zeiss LSM-510 META confocal microscope using a 63×, 1.4 NA (oil) Plan apochromate lens. Fresh hRBCs (6% in PBS) as used in the peptide hemolytic activity assays were incubated with the same concentration of either Rho-labeled BMAP-27 or Rho-Mu-1 BMAP-27 and Rho-Mu-4 BMAP-27 for 15 min at 37 °C. Cells were washed and fixed with 2% paraformaldehyde (10 min) after being extensively washed with PBS, and then confocal microscopic images of cells were taken with an argon ion laser set for Rho excitation at 561 nm. The setting of the photomultiplier was constant during all the experiments.

Localization and binding of the peptides onto the bacterial cells were also examined with the help of Rho-labeled peptides by employing a confocal microscope. *E. coli* cells (~10^6 CFU/mL) in LB medium were incubated in the absence and presence of Rho-labeled BMAP-27 and its analogues at their MICs for 0.5 h and then centrifuged, washed, and analyzed with the confocal microscope as described above.

Fluorescence Energy Transfer Experiments with the Live Cells. FRET experiments were performed by utilizing the NBD- and Rho-labeled peptides on live hRBCs and *E. coli* and analyzed by flow cytometry as reported previously (*45*) with the excitation and emission wavelengths set at 488 and 533 nm, respectively, for NBD. Equimolar amounts of NBD-labeled and unlabeled peptide (donor) and Rho-labeled peptide (acceptor) were added to the hRBCs (~3×10^7 cells/mL) and *E. coli* (~5×10^5 CFU/mL) and incubated at 37 °C for 30 and 10 min, respectively. In FRET experiments, the fluorescence of a particular kind of cells in the presence of NBD-labeled peptide (donor) and unlabeled peptide (U) was compared to the fluorescence of the cells that was recorded in the presence of NBD-labeled peptide and the corresponding Rho-labeled peptide (acceptor).

The percentage of energy transfer exhibited by a peptide for a particular cell was calculated by the following equation.

$$E = [(F_{D+U} - F_{D+A})/F_{D+U}] \times 100$$

where E is the percentage of energy transfer, F_{D+U} is the fluorescence of the cells in the presence of the NBD-labeled peptide (D) and the unlabeled peptide (U), and F_{D+A} is the fluorescence of the cells in the presence of the NBD-labeled peptide and the corresponding Rho-labeled peptide (A).

Confocal Microscopy Experiments To Detect the Self-Assembly of Peptides on Bacteria and hRBCs. To analyze the molecular proximity (aggregation) of NBD and Rho-labeled peptides onto live RBCs and *E. coli*, by confocal microscopy (*46*−*49*) these cells were plated on a poly-L-lysine-coated glass surface for adherence. To include a greater number of bacteria in the experiment of self-assembly of these peptides, *E. coli* ATCC 10536 was employed in this experiment. Equimolar amounts of NBD-labeled or unlabeled peptide (donor) and Rho-labeled peptide (acceptor) were added to the hRBCs (~3×10^7 cells/mL) and *E. coli* (~5×10^5 CFU/mL), incubated at 37 °C for 30 and 10 min, respectively, and washed vigorously with PBS. Confocal microscopic images were scanned by using a Zeiss LSM-510 META confocal microscope using a 63×, 1.4 NA (oil) Plan apochromate lens. Images were scanned by adjusting offset and voltage gain of NBD (excitation, 488 nm) and rhodamine (excitation, 561 nm) fluorescence. The appropriate bandpass was selected to record images. Prebleach NBD and Rho images were collected simultaneously following excitation at 488 nm for NBD (10.1% for *E. coli* and 9.1% for RBC laser intensity) and excitaion at 561 nm for Rho (8.1% for *E. coli* and 7.1% for RBC laser intensity). The selected regions of interest were irradiated with the 561 nm laser line (100% intensity, 100 iterations, using a 488 nm/561 nm dual dichroic mirror) to photobleach rhodamine. Postbleach NBD and rhodamine images were collected simultaneously immediately following photobleaching in line mode. FRET was assessed as an increase in NBD fluorescence intensity following rhodamine photobleaching. The acceptor photobleaching method was used to assess FRET in NBD- and rhodamine-labeled peptides. Colocalization of NBD and rhodamine led to yellow color in the merged images and served as the plausible site for selection of the ROI (region of interest) for acceptor photobleaching. Scattered and random sites in a field were chosen as ROIs for each scan. Imgaes before acceptor photobleaching were recorded as a prebleaching control experiment; 100% laser power was endowed for the efficient acceptor photobleaching. Two scan images after photobleaching was set to record by the software. FRET efficiency was considered positive when the fluorescence intensity of the donor postbleaching was greater than the fluorescence intensity of the donor prebleaching. The following formula was utilized to calculate FRET efficiency: FRET efficiency = (fluorescence intensity of the donor postbleaching − fluorescence intensity of the donor prebleaching)/(fluorescence intensity of the donor postbleaching) × 100.

RESULTS

Design of BMAP-27 Analogues. The phenylalanine zipper sequence has recently been reported in a protein (*50*), which possesses a phenylalanine residue in place of leucine in the leucine zipper sequence. The **a** and **d** amino acids of leucine or phenylalanine zipper sequences play a crucial role in the assembly of proteins or peptides by participating in the intermolecular side chain interactions. Thus, the substitution of amino acids at **a** and **d** positions provides a suitable way to introduce structural changes into the proteins and peptides having these sequences and also to look into its implications in the functional activity of the molecules. To assess the role of the phenylalanine or leucine zipper sequences, amino acids at the **a** and/or **d** position of these heptads were substituted with alanine (Table 1). Alanine was chosen since it is known to abrogate the assembly and oligomeric properties of a protein when it is placed instead of a leucine or isoleucine at the **a** and/or **d** position of the heptads. Moreover, since it is a hydrophobic amino acid, the amphipathic properties of the original peptide are maintained to a large extent. Among the designed analogues, the first two possess a single phenylalanine or leucine residue substituted with alanine, while in the other two analogues, two phenylalanine or leucine residues in **a** or **d** positions were replaced with two alanine residues.

Table 1: Amino Acid Sequences of BMAP-27 and Its Analogues

Peptides	**Amino acid sequences** (X=H, NBD or Rhodamine) (Amino acids at 'a' and 'd' positions are bold and substituted amino acids are boldface and underlined)
	f g a b c d e f g a b c d e f g a b c d e f g a b c
BMAP-27	X-NH- G R **F** K R **F** R K K **F** K K **L** F K K **L** S P **V** I P L **L** H L -$CONH_2$
Mu-1 BMAP-27	X-NH- G R **F** K R **F** R K K **A** K K **L** F K K **L** S P **V** I P L **L** H L -$CONH_2$
Mu-2 BMAP-27	X-NH- G R **F** K R **F** R K K **F** K K **L** F K K **A** S P **V** I P L **L** H L -$CONH_2$
Mu-3 BMAP-27	X-NH- G R **A** K R **F** R K K **A** K K **L** F K K **L** S P **V** I P L **L** H L -$CONH_2$
Mu-4 BMAP-27	X-NH- G R **F** K R **F** R K K **F** K K **A** F K K **A** S P **V** I P L **L** H L -$CONH_2$

Table 2: Antibacterial Activities of BMAP-27 and Its Analogues

	minimal inhibitory concentration (MIC)[a] (μM)			
peptide/antibiotic	*S. aureus* ATCC 9144	*B. subtilis* ATCC 6633	*E.coli* DH5α	*E. coli* ATCC 10536
BMAP-27	2.7 ± 0.8	2.6 ± 0.7	2.8 ± 0.6	3.2 ± 0.9
Mu-1 BMAP-27	2.8 ± 0.8	2.7 ± 0.7	2.9 ± 0.6	3.2 ± 0.9
Mu-2 BMAP-27	2.8 ± 0.8	2.7 ± 0.7	2.9 ± 0.6	2.9 ± 0.9
Mu-3 BMAP-27	2.7 ± 0.8	2.8 ± 0.7	2.9 ± 0.8	2.9 ± 0.9
Mu-4 BMAP-27	2.7 ± 0.8	2.9 ± 0.7	2.9 ± 0.6	2.7 ± 0.9
tetracycline	1.0 ± 0.2	1.0 ± 0.2	1.2 ± 0.2	1.2 ± 0.9

[a]MIC values are the means of three independent experiments each performed in duplicate ± the standard deviation.

BMAP-27 and Its Analogues Exhibit Similar and Appreciable Antibacterial Activity. To determine the antibacterial activity of BMAP-27 and its analogues, peptides were tested for growth inhibiting activity in liquid cultures against Gram-positive and Gram-negative bacteria. Tetracycline was used as a positive control. Interestingly, the antibacterial activities of alanine-substituted analogues were close to that of BMAP-27 (Table 2). The results showed that the antibacterial activity of BMAP-27 was almost intact after the substitution of leucine/phenylalanine residue(s) with alanine residue(s) in its **a** and/or **d** position of the leucine/phenylalanine zipper sequence. Antibacterial activities of these peptides were evaluated against one Gram-positive bacterium (*B. subtilis* ATCC 6633) and one Gram-negative bacterium (*E. coli* ATCC 10536) in the presence of serum. BMAP-27 and its analogues exhibited comparable bactericidal activity against these selected bacteria in the presence of serum (Table 1 of the Supporting Information). However, the MIC values of the peptides in the presence of serum against *E. coli* ATCC 10536 were approximately double that in the absence of serum, while the MIC values against *B. subtilis* ATCC 6633 in the presence of serum were ~4 times that in the absence of serum. The data indicated that serum proteins inhibited the antibacterial activity of BMAP-27 and its analogues against these selected bacteria to varying degrees. Furthermore, bactericidal activities of these Rho-labeled peptides were assayed against the selected Gram-positive and Gram-negative bacteria (Figure 1 of the Supporting Information), which suggested that Rho labeling did not significantly affect the activity of BMAP-27 and its analogues.

*Alteration of the Cytotoxic Activity of BMAP-27 after Substitution of Phenylalanine or Leucine with Alanine at the **a** and/or **d** Position of Phenylalanine and Leucine Zipper Sequences*. The cytotoxic activity of BMAP-27 and its analogues was determined by measuring their hemolytic activity against the human red blood cells and the viability of murine 3T3 cells in their presence. BMAP-27 exhibited the maximum hemolytic activity against hRBCs (Figure 1A). However, the hemolytic activity was drastically reduced in the BMAP-27 analogues in which single or double phenylalanine or leucine residues were replaced with alanine. Thus, the data clearly suggested that these phenylalanine or leucine residues at the **a** and/or **d** position of the BMAP-27 heptads play a crucial role in maintaining the hemolytic activity of the peptide.

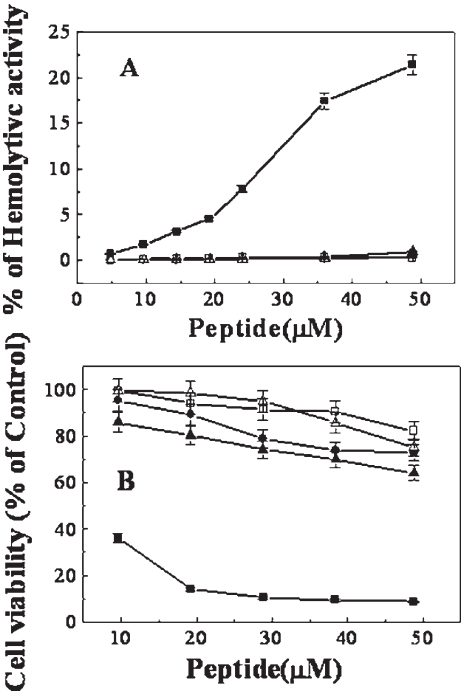

FIGURE 1: Decrease in the toxic activity of BMAP-27 against hRBC and murine 3T3 cells after substitution of leucine and/or phenylalanine residues at the **a** and/or **d** position with alanine. (A) Dose-dependent hemolytic activity assay of BMAP-27 (■), Mu-1 BMAP-27 (●), Mu-2 BMAP-27 (○), Mu-3 BMAP-27 (▲), and Mu-4 BMAP-27 (△). (B) Dose-dependent MTT assay of 3T3 cells in the presence of BMAP-27 (■), Mu-1 BMAP-27 (●), Mu-2 BMAP-27 (○), Mu-3 BMAP-27 (▲), and Mu-4 BMAP-27 (△). Each point represents the mean result of three independent experiments, and the error bar indicates the standard deviation.

The viability of 3T3 cells in the presence of BMAP-27 and its analogues was detected by measuring the mitochondrial dehydrogenese activity of these cells with a MTT assay. 3T3 cells were least viable in the presence of BMAP-27 as compared to the other peptides, indicating the higher cytotoxicity of the wild-type peptide versus its analogues. Thus, the designed analogues with substitution of phenylalanine or leucine in the phenylalanine or leucine zipper sequences exhibited a similar trend in the reduction

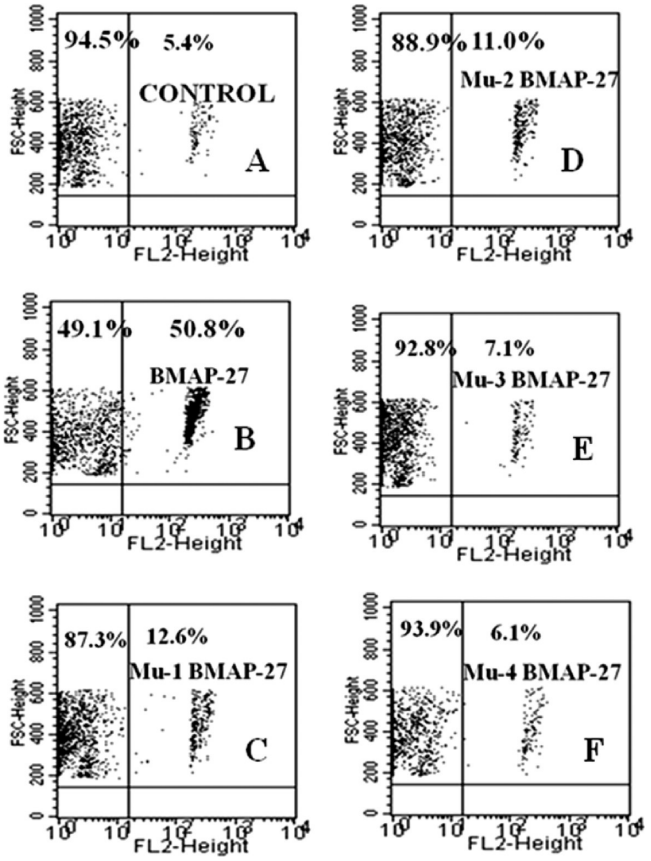

FIGURE 2: Determination of peptide-induced membrane damage of murine 3T3 cells by flow cytometric studies. Panels A−F show the PI staining of untreated murine 3T3 cells and cells treated with ~10.0 μM BMAP-27, Mu-1 BMAP-27, Mu-2 BMAP-27, Mu-3 BMAP-27, and Mu-4 BMAP-27, respectively. On the *Y* axis, FSC-Height is the forward scattered height which shows the distribution of the cells. On the *X* axis, FL2-Height means the fluorescence recorded by fluorescent filter 2 (red channel). Ten thousand events were counted for each experiment.

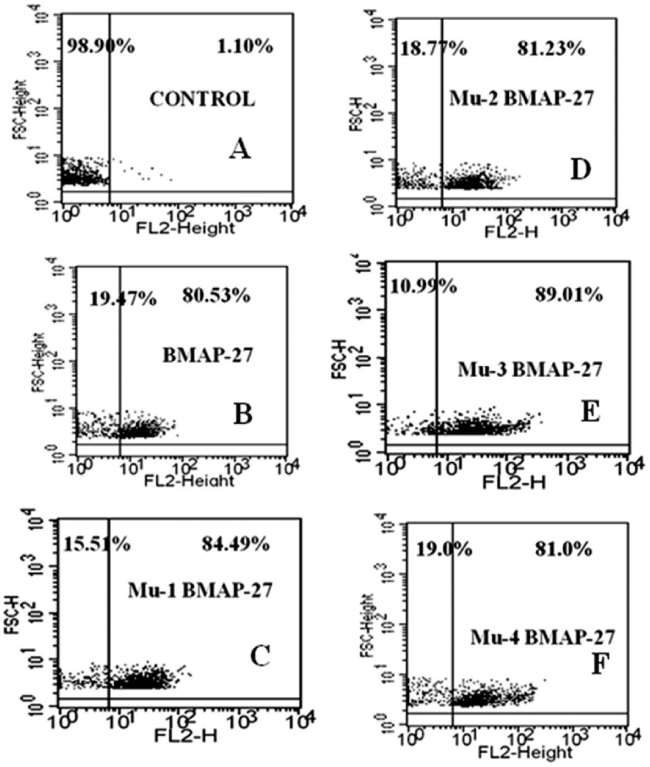

FIGURE 3: Determination of the peptide-induced membrane damage of *E. coli* cells by flow cytometric studies. Panels A−F show the PI staining of untreated *E. coli* cells and cells treated with ~3.5 μM BMAP-27, Mu-1 BMAP-27, Mu-2 BMAP-27, Mu-3 BMAP-27, and Mu-4 BMAP-27, respectively. On the *Y* axis, FSC-Height (*H*) means the forward scattered height that shows the distribution of the cells. On the *X* axis, FL2-Height means the fluorescence recorded by fluorescent filter 2 (red channel). Ten thousand events were counted for each experiment.

of cytotoxicity against the 3T3 cells (Figure 1B), which was observed in the case of determining their hemolytic activity against the hRBCs. The results thus suggested that the substitution of phenylalanine and leucine at the **a** and/or **d** position in the phenylalanine or leucine zipper sequence altered the toxic activity of BMAP-27 not only against the hRBCs but also against the mouse fibroblast 3T3 cells, probably implicating these sequences in the maintenance of the cytotoxic activity of this antimicrobial peptide. Altogether, the data indicate a possible role of both leucine and phenylalanine zipper sequences in the cytotoxic activity of BMAP-27.

Unlike BMAP-27, Its Analogues Selectively Damaged the Membrane Organization of Bacteria but Not the Mammalian Cells. The changes in membrane organization of murine fibroblast 3T3 cells and bacteria, *E. coli*, in the presence of BMAP-27 and its analogues were probed by incubation of the peptide-treated cells with the DNA intercalating dye propidium iodide (PI). PI is impermeable to normal viable cells, and it can enter only those cells and interact with their DNA whose membranes are damaged. PI staining of 3T3 cells following the treatment of the peptides showed that BMAP-27 damaged the membrane organization of these cells to the highest extent, while its analogues were appreciably less active (Figure 2).

However, interesting results were obtained when *E. coli* cells were stained with PI following the treatment of BMAP-27 and its alanine-substituted analogues. Unlike in the case of PI staining of 3T3 cells after the treatment of the peptides, *E. coli* cells treated with either BMAP-27 (3.5 μM) or its analogues exhibited an almost similar shift (~80%) of the dots to the upper right side (Figure 3), indicating similar damage of the membrane organization of the bacteria by each of these peptides. The data suggested that the substitution of phenylalanine and leucine with alanine in the phenylalanine and leucine zipper motifs, respectively, impaired the ability of BMAP-27 only to damage the membrane organization of 3T3 cells but not bacteria, *E. coli*. Furthermore, peptide-induced membrane damage of *E. coli* ATCC 10536 was studied in the presence of the NBD-labeled BMAP-27 and its selected alanine-substituted analogue and compared with the damage induced by their unlabeled versions (Figure 1 of the Supporting Information). The results indicated that no significant difference was observed between the membrane damage caused by the unlabeled peptide and that caused by the corresponding unlabeled version.

Contrasting Differences between BMAP-27 and Its Analogues in Depolarizing hRBCs while These Peptides Depolarized E. coli to a Similar Extent. Membrane depolarization of bacterial, *E. coli*, and mammalian, hRBCs, membranes was assessed in the presence of BMAP-27 and its analogues to improve our understanding of the possible mode of action and the molecular basis of their contrasting cytotoxic activity but very similar antibacterial activity. Depolarization of *E. coli* and hRBC membranes induced by BMAP-27 and its analogues was assessed with the help of a potential sensitive dye diS-C_3-5. Depolarization

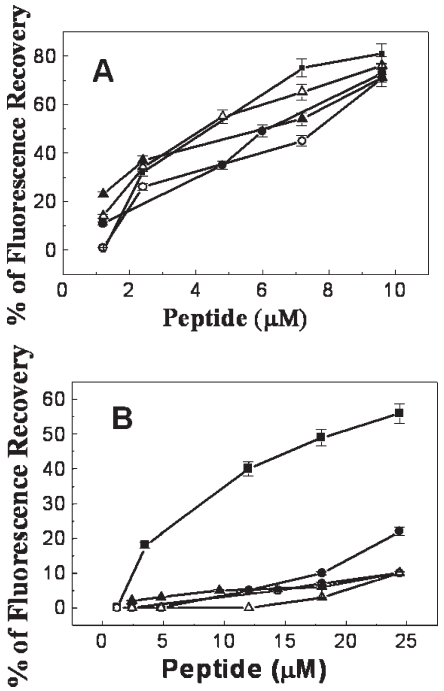

FIGURE 4: Dose-dependent peptide-induced transmembrane depolarization of *E. coli* and hRBC. (A and B) Plots of the percentage of fluorescence recovery, which is a measure of transmembrane depolarization, vs peptide concentration (micromolar) of *E. coli* and hRBCs, respectively: (■) BMAP-27, (●) Mu-1 BMAP-27, (○) Mu-2 BMAP-27, (▲) Mu-3 BMAP-27, and (△) Mu-4 BMAP-27. Each point represents the mean result of three independent experiments, and the error bar indicates the standard deviation.

of each of these cell membranes in the presence of BMAP-27 and its analogues was assessed with respect to fluorescence recovery induced by these peptides at different concentrations as described in Materials and Methods. BMAP-27 and its analogues induced very similar membrane depolarization in *E. coli* (Figure 4A), as indicated by the similar fluorescence recovery induced by these peptides. However, the alanine-substituted analogs of BMAP-27 induced significantly lower membrane depolarization in hRBCs compared to that of wild type BMAP-27 (Figure 4B). Thus, the results indicated that although the substitution of leucine or phenylalanine with alanine had an almost negligible effect on the peptide-induced depolarization in *E. coli* it significantly impaired the BMAP-27-induced depolarization of the hRBC membrane.

Differences between BMAP-27 and Its Analogues in Permeabilizing the Zwitterionic Lipid Vesicles but Not in Negatively Charged Lipid Vesicles. Often lipid vesicles with zwitterionic (like PC/Chol) and negatively charged lipids (like PE/PG or PC/PG) are employed to mimic the eukaryotic and prokaryotic cell membrane, respectively. Therefore, to understand the basis of differences and similarities in BMAP-27 and its alanine-substituted analogues induced by depolarization of hRBCs and bacteria, respectively, permeabilization of both zwitterionic PC/Chol and negatively charged PC/PG vesicles in the presence of these peptides was examined by measuring the peptide-induced depolarization of these lipid vesicles as described in Materials and Methods. The increase in the fluorescence of the probe, which resulted from the dissipation of diffusion potential across the membrane, indicated the peptide-induced permeability of a particular kind of lipid vesicles. Figure 5A shows experimental profiles of depolarization of PC/Chol vesicles by BMAP-27 and its analogues at a particular peptide concentration, while the plot of fluorescence recovery, which is a measure of peptide-induced permeabilization of these lipid vesicles versus peptide concentration, is presented in Figure 5C. It is evident from the fluorescence enhancement of the probe following the addition of the peptides that wild-type BMAP-27 appreciably permeabilized PC/Chol vesicles. However, all the single and double alanine-substituted analogues were significantly less active than the wild-type molecule, clearly suggesting that alanine substitution significantly impaired the ability of BMAP-27 to permeabilize the zwitterionic lipid vesicles. Interestingly, contrasting results were observed when the depolarization of negatively charged lipid vesicles was measured in the presence of these peptides. As is evident from the representative fluorescence profiles at a particular peptide concentration (Figure 5B) and the plot of fluorescence recovery versus peptide concentration (Figure 5D), BMAP-27 and its analogues possess significant and almost similar efficacy in permeabilizing the PC/PG lipid vesicles.

To further characterize BMAP-27- and analogue-induced permeability of zwitterionic and negatively charged lipid vesicles, release of calcein from both kinds of calcein-entrapped lipid vesicles in the presence of these peptides was examined. BMAP-27 appreciably induced release of calcein from calcein-entrapped zwitterionic PC/Chol and negatively charged PC/PG lipid vesicles as evidenced by the representative calcein release profiles (Figure 2A,B of the Supporting Information) and the plot of fluorescence recovery data (Figure 2C,D of the Supporting Information). On the other hand, alanine-substituted BMAP-27 analogues were as efficient as the wild-type molecule in releasing calcein from calcein-entrapped PC/PG lipid vesicles [profiles at a particular concentration (Figure 2B of the Supporting Information) and fluorescence recovery plot (Figure 2D of the Supporting Information)]. However, as in the membrane depolarization study, these analogues induced the release of calcein from zwitterionic PC/Chol vesicles to a much lesser extent than BMAP-27 [calcein release profiles (Figure 2A of the Supporting Information) and fluorescence recovery plot (Figure 2C of the Supporting Information)]. Altogether, the results of membrane depolarization and release of calcein from calcein-entrapped lipid vesicles indicated that the alanine-substituted BMAP-27 analogues induced a reduced level of permeabilization only in zwitterionic lipid vesicles and not in the negatively charged lipid vesicles.

Induction of the α-Helical Structure of BMAP-27 and Its Analogues in the Membrane Mimetic Environments. Circular dichroism (CD) experiments were performed to study the secondary structures of BMAP-27 and its analogues in an aqueous environment [phosphate-buffered saline (PBS) (pH 7.4)] and in the membrane mimetic environments like SDS micelles and 40% TFE (v/v, in water). The peptides did not adopt significant helical structures in PBS (data not presented). However, in both 40% TFE and 1% SDS, BMAP-27 and its analogues adopted appreciable helical structures, which is evident from the shape of the spectra (Figure 6). Considering the mean residue ellipticity values at 222 nm, it appears that in 40% TFE BMAP-27 and it analogues adopted 30−45% helical structures whereas in 1% SDS the peptides were 33−43% helical.

Significant Difference in the ANS Fluorescence of BMAP-27 and Its Analogues. ANS is a hydrophobic fluorescent probe, which is practically nonfluorescent in an aqueous environment. However, in a hydrophobic environment, its

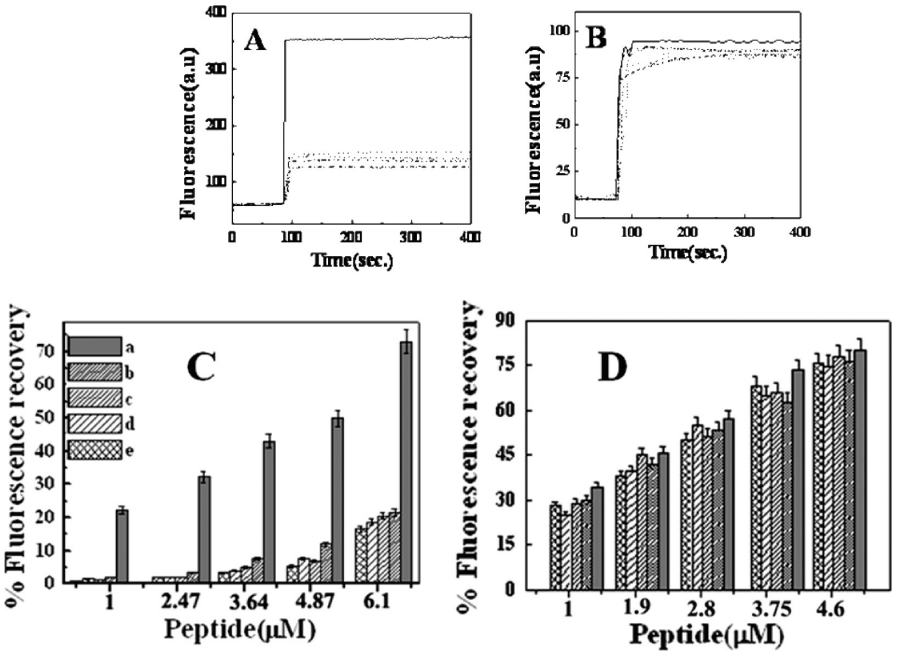

FIGURE 5: Permeabilization of zwitterionic and negatively charged lipid vesicles by BMAP-27 and its analogues as studied by the dissipation of diffusion potentials induced by the individual peptides. (A) Profiles of dissipation of diffusion potential of zwitterionic PC/Chol lipid vesicles in the presence of BMAP-27 and its analogues with peptide concentration for each of the peptides at ~6.1 μM. (B) Profiles of dissipation of diffusion potential of negatively charged PC/PG lipid vesicles induced by BMAP-27 and its analogues with peptide concentration for each of the peptides at ~4.6 μM. Symbols for panels A and B: BMAP-27 (—), Mu-1 BMAP-27 (---), Mu-2 BMAP-27 (· · ·), Mu-3 BMAP-27 (-·-), and Mu-4 BMAP-27 (-· · ·). (C and D) Column plots of fluorescence recovery induced by BMAP-27 and its analogues in PC/Chol and PC/PG lipid vesicles, respectively. All the peptides were employed at five equal but different concentrations as marked on the *X* axis. Columns a−e depict data for BMAP-27, Mu-1 BMAP-27, Mu-2 BMAP-27, Mu-3 BMAP-27, and Mu-4 BMAP-27, respectively. The concentration of PC/Chol and PC/PG lipid vesicles was 68 μM. Each point represents the mean result of three independent experiments, and the error bar indicates the standard deviation.

fluorescence is significantly enhanced with the shift in the emission maximum to a shorter wavelength. Self-association of BMAP-27 and its analogues in an aqueous environment was probed by ANS as reported previously (*44*). In PBS, ANS showed negligible fluorescence. However, in the presence of BMAP-27, the fluorescence of ANS increased significantly with an emission maximum at a shorter wavelength at ~485 nm, indicative of binding of the probe to the hydrophobic peptide environment which probably resulted from the aggregation of the peptide (Figure 3 of the Supporting Information). Interestingly, a totally distinct result was observed when ANS fluorescence was recorded in the presence of BMAP-27 analogues. Singly and doubly alanine-substituted BMAP-27 analogues induced much less enhancement of ANS fluorescence and a smaller shift of its emission maximum (~500.5 nm) toward the shorter wavelength as compared to that observed for the parent molecule (Figure 3 of the Supporting Information). The data clearly indicate that BMAP-27 was much more self-aggregated than its alanine-substituted analogues in an aqueous environment. In other words, substitution of leucine and phenylalanine with alanine in the corresponding zipper sequences disturbed the self-association of BMAP-27. Interestingly, a scrambled BMAP-27 analogue (SCR-BMAP-27) having the same amino acid composition as BMAP-27 with an only minor alteration in the zipper sequences also induced a smaller shift toward a shorter wavelength (emission maximum at ~494 nm) and significantly less enhancement of the fluorescence of ANS than in the presence of BMAP-27, suggesting a possible role of these zipper sequences in the self-association of BMAP-27 in an aqueous environment.

Contrasting Localization of BMAP-27 and Its Analogues onto hRBC Cells but Not in Bacteria. The effect of substitution of leucine and phenylalanine with alanine in the leucine and phenylalanine zipper sequences, respectively, of BMAP-27 on its localization onto hRBCs was studied (left-hand side, Figure 7) by confocal microscopy. Bright red fluorescence of Rho-BMAP-27 was observed for the hRBCs, indicating strong binding of BMAP-27 molecules to these cells. However, the hRBCs after incubation with Rho-Mu-1 BMAP-27 exhibited much weaker fluorescence, and the cells after treatment with Rho-Mu-4 BMAP-27 exhibited the least fluorescence. The data clearly suggest that substitution of phenylalanine and leucine residue(s) with alanine residue(s) in the BMAP-27 heptad progressively disturbed the binding and localization of the molecule onto the human red blood cells.

Interestingly, while looking at the localization of these peptides onto the bacteria, we observed strong red fluorescence of Rho-BMAP-27 as well as its Rho-labeled alanine-substituted analogues on the *E. coli* cells (right-hand side, Figure 7). Thus, confocal microscopy studies showed a similar binding and localization of BMAP-27 and its analogues onto bacteria when treated at ~70% of the MIC concentrations. Moreover, when confocal microscopic images of *E. coli* were recorded after treatment with the Rho-labeled peptides at MIC concentrations, damage of the bacterial cell membrane with a change in their morphology was observed. The data clearly indicate that these peptides targeted the bacterial membrane and further suggest that Rho labeling did not disturb the activity of these peptides against the bacteria. Taken together, confocal microscopy studies revealed that the substitution of leucine and phenylalanine with alanine in the leucine and phenylalanine zipper sequences, respectively, had a significant effect on the binding and localization of BMAP-27 onto the hRBC cells, although it had a negligible influence on the localization of the peptide onto *E. coli* cells.

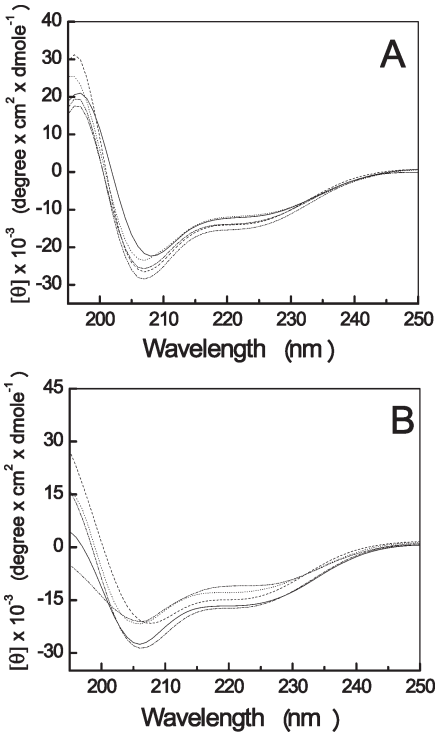

FIGURE 6: Determination of secondary structures of 21.0 μM BMAP-27 and its analogues in the presence of 40% TFE (v/v, in water) (A) and 1% SDS (B): BMAP-27 (—), Mu-1 BMAP-27 (---), Mu-2 BMAP-27 (···), Mu-3 BMAP-27 (-·-), and Mu-4 BMAP-27 (-···).

Alanine-Substituted BMAP-27 Analogues Adopted Weaker Assembly on hRBCs while They Assembled as Well as BMAP-27 on E. coli. The role of assembly of antimicrobial peptides on bacteria and mammalian cells in determining their antibacterial and cytotoxic activities is not well understood. Toward this end, the assembly of BMAP-27 and its selected analogues on the live hRBCs and *E. coli* was examined with the help of fluorescence resonance energy transfer experiments by employing NBD- and Rho-labeled versions of the peptides as energy donors and acceptors, respectively. The fluorescence of *E. coli* and hRBCs in the presence of different fluorescently labeled peptides was measured by a flow cytometer. NBD-BMAP-27 appreciably bound to the hRBCs as indicated by the significant fluorescence levels (*X* axis value) of these cells (Figure 8) when incubated with the labeled peptide. However, when Rho-labeled BMAP-27 was added to NBD-BMAP-27-bound hRBCs, appreciable energy transfer was observed as evidenced by the decrease in the NBD fluorescence of these cells (the shift in the fluorescence peak toward the left-hand side, lower value). Thus, the data suggested that BMAP-27 self-assembled on the hRBC cells (Figure 8). In contrast, the binding of both the NBD-labeled alanine-substituted analogues, Mu-1 BMAP-27 and Mu-4 BMAP-27, was appreciably weaker than that of wild-type BMAP-27 as indicated by the less intense fluorescence level (the *X* axis value) of the cells in their presence. Furthermore, the decrease in NBD fluorescence of the hRBCs when these unlabeled BMAP-27 analogues were replaced with their Rho-labeled version was smaller than that observed in the case of wild-type NBD-BMAP-27, indicating weaker energy transfer events between the donor- and acceptor-labeled BMAP-27 analogues as compared to that of wild-type BMAP-27. Thus, the results indicated that the alanine-substituted BMAP-27

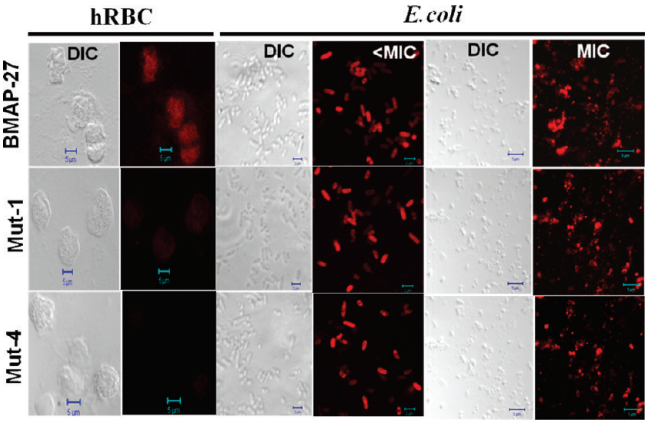

FIGURE 7: Detection of localization of the Rho-labeled BMAP-27, Rho-labeled Mu-1 BMAP-27, and Rho-labeled Mu-4 BMAP-27 onto hRBCs and *E. coli* DH5α by confocal microscopy. Each cell type has been marked at the top of the figure, and Rho-labeled peptides, BMAP-27, Mu-1 BMAP-27 (in short Mut-1), and Mu-4 BMAP-27 (in short Mut-4), that have been used to treat the cells are shown on the left-hand side. For each peptide treatment, fluorescence and DIC images of each cell type are shown. The peptide concentration of each of the Rho-labeled peptides for treatment with hRBCs was ~12 μM, whereas for treatment with *E. coli* below the MIC the concentration was ~2.0 μM and at the MIC was ~3.0 μM. hRBCs were plated on a poly-L-lysine-coated slide and incubated with rhodamine-labeled peptides for 15 min in PBS. Afterward, cells were fixed in 2% paraformaldehyde (10 min) and washed extensively with PBS. Before confocal scanning (oil immersion, 63×, crop size of 2), slides were mounted with 80% glycerol containing antifade. Similarly, log phase *E. coli* cells were incubated with rhodamine-labeled peptides for 15 min at different concentrations (MIC and 70% of MIC) and placed on poly-L-lysine-coated slides. Afterward, cells were fixed with 2% paraformaldehyde (10 min) and washed extensively. Before confocal scanning (oil immersion, 63×, crop size of 2), the samples were mounted with 80% glycerol containing antifade.

analogues did not self-assemble appreciably on live hRBC cells unlike their parent molecule. Interestingly, when the assembly of BMAP-27 and its two selected analogues was examined on live *E. coli* in a similar way by fluorescence energy transfer experiments, both BMAP-27 and its alanine-substituted analogues exhibited appreciable and comparable self-assembly on the bacteria (right-hand side, Figure 8). This is evidenced by the observation that for all three peptides, the NBD fluorescence of *E. coli* cells decreased appreciably following the addition of the corresponding Rho-labeled peptide in place of the respective unlabeled peptide. A quantitative analysis of these FRET experiments was performed by utilizing the mean fluorescence of the cells in the presence of the NBD-labeled peptide and the corresponding unlabeled peptide (F_{D+U}) and the mean fluorescence of the cells in the presence of NBD- and Rho-labeled peptides (F_{D+A}), described in Materials and Methods. As shown in Figure 8G, BMAP-27 showed an energy transfer of ~31% on hRBCs whereas the selected analogues (Mu-1 BMAP-27 and Mu-4 BMAP-27) showed only 4 and 2% energy transfer, respectively, on the same cells indicating a significant difference between the wild-type and mutant peptides in their self-assembly on hRBCs. In contrast, all three peptides exhibited appreciable and very similar energy transfer (~55%), suggesting that all these peptides self-assembled to a similar extent on *E. coli* unlike in the case of hRBCs.

Self-assembly of BMAP-27 and its analogues was further probed by confocal microscopy studies (*46*, *47*) via examination of the enhancement of donor (NBD-labeled peptide) fluorescence

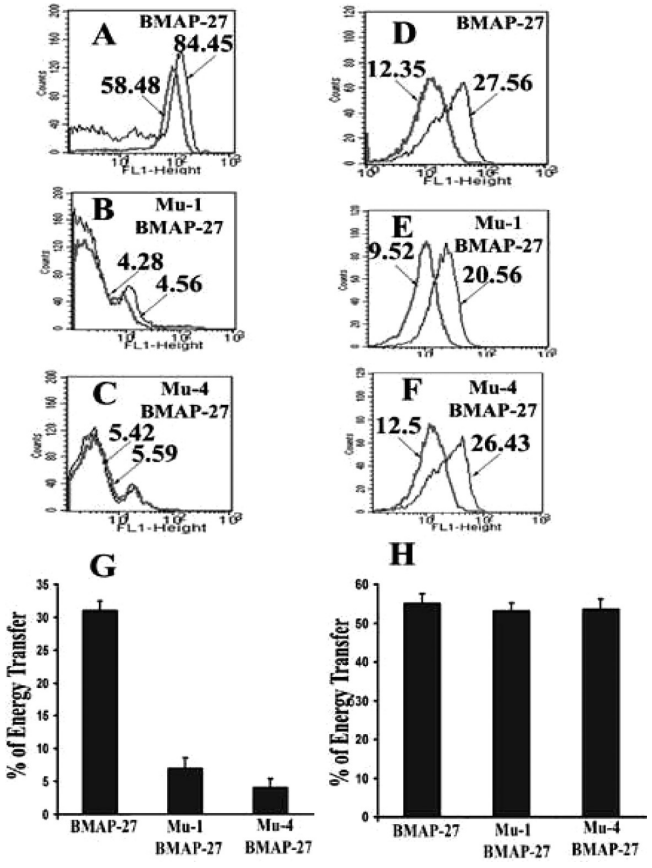

FIGURE 8: Detection of self-assembly of BMAP-27, Mu-1 BMAP-27, and Mu-4 BMAP-27 on *E. coli* and hRBCs by FRET experiments with the help of flow cytometry. Equimolar amounts of NBD-labeled peptides (D) and either the corresponding unlabeled peptide (U) or Rho-labeled peptide (A) incubated with hRBCs (A−C) and *E. coli* cells (D−F) at 37 °C and then analyzed by flow cytometry. Black (thinner) and gray (thicker) lines represent (D + U) and (D + A), respectively. (A−C) FRET experiments on hRBCs with BMAP-27, Mu-1 BMAP-27, and Mu-4 BMAP-27, respectively, with each of the peptides at ~12.0 μM. (D−F) FRET experiments on *E. coli* cells with the same peptides at ~3.0 μM. The numerical values shown on the profiles represent the mean fluorescence intensities. Ten thousand events were counted for each of these experiments. (G and H) Percentage of energy transfer (described in Materials and Methods) observed with different peptides as marked in the figure on hRBCs and *E. coli*, respectively. Each percent of FRET value represents the mean result of two independent experiments, and the error bar indicates the standard deviation.

as a result of photobleaching of the acceptor molecule (corresponding Rho-labeled peptide) on *E. coli* and hRBCs (Figure 4 of the Supporting Information). A significant increase in the NBD fluorescence at the site of acceptor photobleaching was observed for both BMAP-27 and its analogues on *E. coli* (Figure 4A,B of the Supporting Information). The data clearly indicate energy transfer between NBD and Rho-labeled BMAP-27 as well as its analogues resulting from the self-assembly of these individual peptide molecules on *E. coli*. However, similar energy transfer experiments on hRBCs revealed self-association of only wild-type BMAP-27 (Figure 4C,D of the Supporting Information). BMAP-27 analogues bound very weakly to hRBCs and did not self-assemble appreciably on hRBCs (Figure 4C,D of the Supporting Information). Altogether, confocal microscopy studies supported the trend of the data from FRET experiments by flow cytometry on live *E. coli* and hRBCs.

DISCUSSION

The results show the identification and characterization of a small stretch of phenylalanine and a leucine zipper sequence at the N- and C-termini of a long heptad repeat in bovine antimicrobial peptide BMAP-27. It is evident from the data that the substitution of either phenylalanine or leucine at the **a** and/or **d** position of phenylalanine or leucine zipper sequences severely reduced the toxic activity of BMAP-27 without affecting its antimicrobial activity. The results clearly suggested the role of these sequences in maintaining the cytotoxic activity of cathelicidin-derived bovine antimicrobial BMAP-27 peptides. A decrease in the bactericidal activity of BMAP-27 and its analogues versus the selected bacteria in the presence of serum (Table 1 of the Supporting Information) indicated interference by plasma proteins toward the antimicrobial activity of the peptides as was also observed in the case of LL-37 (*51*). Labeled peptides retained the antibacterial activity against the bacteria and also damaged their membrane organization like their unlabeled versions, suggesting that labeling of BMAP-27 and its analogues did not disturb their functional activities (Figure 1 of the Supporting Information). To explore further evidence of the role of these zipper sequences in maintaining the cytotoxicity of BMAP-27, a scrambled BMAP-27 analogue (SCR-BMAP-27) that possesses the same amino acid composition as the original peptide except for a minor alteration in the zipper sequence was designed (Figure 5 of the Supporting Information). The positions of polar and charged residues in this analogue were the same as in the wild-type peptide. Since SCR-BMAP-27 possesses the same amino acid composition as the wild-type peptide and only the positions of the hydrophobic amino acids were interchanged with each other to include a minor modification in the leucine and phenylalanine zipper sequences, this analogue retains the amphipathic properties of BMAP-27. Helical wheels of BMAP-27, SCR-BMAP-27, and a doubly alanine-substituted analogue (Mu-3 BMAP-27) are shown in Figure 5 of the Supporting Information. However, despite having the same amino acid composition as BMAP-27, SCR-BMAP-27 exhibited drastically reduced hemolytic activity against hRBCs and cytotoxicity against 3T3 cells (Figure 5 of the Supporting Information), confirming the crucial role of the leucine and phenylalanine zipper sequences in maintaining the cytotoxicity of BMAP-27, yet SCR-BMAP-27 exhibited antibacterial activity comparable to that of BMAP-27 or its analogues. This peptide damaged the membrane organization of *E. coli* but not of 3T3 cells (Figure 5 of the Supporting Information).

The hydrophobicity of antimicrobial peptides is often utilized to explain the hemolytic activity of the antimicrobial peptides, which is a measure of their cytotoxicity. However, the molecular basis of reduction of the toxicity of an antimicrobial peptide as a result of a decrease in its hydrophobicity is not well-known. The substitution of one and two leucine or phenylalanine residues with alanine will not drastically reduce the hydrophobicity of the 27-residue BMAP-27. However, even after single-amino acid substitution, a drastic reduction in the hemolytic activity of BMAP-27 was observed; practically all the singly or doubly alanine-substituted BMAP-27 analogues showed no detectable hemolytic activity (Figure 1) up to the peptide concentration of ~50 μM used for this experiment. The results clearly suggest that the decrease in the hydrophobicity of BMAP-27 as a result of these amino acid substitutions cannot alone explain the severely reduced toxicity of BMAP analogues. The hemolytic activity

data of SCR-BMAP-27 confirm that just maintaining the composition, hydrophobicity, or amphipathic property is not enough to preserve the cytotoxicity of BMAP-27.

The possible mechanism of action of BMAP-27 and its analogues for killing the microorganisms and mammalian cells was studied by directly looking into the ability of the peptides to depolarize these cells. BMAP-27 depolarized both hRBCs and *E. coli* with significant efficacy, which also matched with its non-cell-selective hemolytic and antibacterial activities. All the alanine-substituted analogues also induced appreciable permeability in the bacteria, which was comparable to that of wild-type BMAP-27. Interestingly, the substitution of phenylalanine or leucine at the **a** and/or **d** position of the phenylalanine or leucine zipper sequence, respectively, drastically reduced the level of BMAP-27-induced depolarization of hRBCs, which probably points toward the basis of the decrease in toxic activity of BMAP-27 analogues versus hRBCs. Propidium iodide (PI) staining of 3T3 and bacterial cells after the treatment of BMAP-27 and its analogues supports the peptide-induced killing and depolarization of these cells.

The flow cytometric studies of PI staining (Figures 2 and 3) and peptide-induced depolarization of *E. coli* and hRBCs (Figure 4) indicate that probably BMAP-27 primarily interacts with the membrane of the target cells to exhibit cytotoxic and antibacterial activities, and peptide-induced permeabilization of the target cells is the key event associated with the killing of these cells. Furthermore, the observation of damage of the cell membrane and the change in morphology by confocal microscopy studies of *E. coli* at the MIC of BMAP-27 (Figure 7) and its analogues supported the possibility that these peptides could target the cell membrane of bacteria to exhibit their antibacterial activity. The ability of BMAP-27 to bind and localize on the cell membrane of both mammalian and bacterial cells probably assists in the permeabilization of both kinds of cell membranes. That substitution of leucine and/or phenylalanine with alanine impaired the localization of BMAP-27 onto the hRBCs, which could contribute to the weak permeability of these cells in the presence of BMAP-27 analogues. The similarities of the results of the membrane permeability studies of selected mammalian cells and bacteria (Figure 4) with the corresponding mimetic lipid vesicles (Figure 5 and Figure 2 of the Supporting Information) probably indicate a key role for lipid−peptide interaction in determining the activity of BMAP-27 and its analogues. Circular dichroism studies (Figure 6) indicated both BMAP-27 and its analogues adopted appreciable helical structures in membrane mimetic environments. Nevertheless, differences between BMAP-27 and its analogues in their self-assembly onto hRBCs but not *E. coli* were observed (Figure 8 and Figure 4 of the Supporting Information), which could significantly contribute in the distinct nature of the peptide-induced permeability of the mammalian cells and bacteria. However, the exact stage of interaction of BMAP-27 or its analogues with the bacterial membrane at which the peptides self-assemble onto bacteria is unclear. We cannot rule out a possibility that these peptide molecules first bind to the surface of bacteria like carpet and then self-assemble with the neighboring molecules in the course of disrupting the bacterial membrane.

Altogether, the data suggest that the substitution of leucine or phenylalanine with alanine in the leucine or phenylalanine zipper sequence of BMAP-27, respectively, impaired the localization and assembly of the peptide on the hRBCs, which could contribute to impairing the ability of BMAP-27 to permeabilize these cells, and therefore, its analogues probably exhibited weak hemolytic activities. In contrast, both BMAP-27 and its analogues exhibited similar binding, localization, and assembly on *E. coli*, which probably resulted in their similar ability to depolarize the bacteria, and thus, the peptides exhibited similar lytic activity against the bacteria. Interesting differences were observed between BMAP-27 and its alanine-substituted analogues in their self-assembly in aqueous PBS. ANS binding (Figure 3 of the Supporting Information) clearly demonstrated that BMAP-27 was significantly more aggregated than its analogues, supporting the role of these zipper sequences in the assembly of a peptide in an aqueous environment as already shown by others for proteins and peptides. Moreover, the fact that the more aggregated peptide is more toxic than the less aggregated peptide in an aqueous environment showed similarity with previous studies (*26*, *27*, *52*).

The molecular basis of assembly of alanine-substituted analogues of BMAP-27 on bacteria is not well-understood. The primary difference between the outer membrane of the mammalian cell and that of the bacterial membrane is that the former contains zwitterionic lipids and is electrically neutral while the latter is negatively charged because of the presence of LPS/lipoteichoic acid and negatively charged lipids. We speculate that the hydrophobic interaction between the adjacent leucine and phenylalanine residues of the leucine and phenylalanine zipper sequences of BMAP-27, respectively, is very crucial for maintaining self-assembly of the peptide on the mammalian cell membrane. Since BMAP-27 is highly positively charged (eight positive charges at physiological pH), the peptide molecules could be attracted to the bacterial membrane. Probably, at some peptide concentration, on the bacterial membrane surface they can come close to each other and self-assemble. Probably, the electrostatic interaction between the cationic residues of the peptides and the negative charge of the bacterial membrane compensates for the loss of the hydrophobic interaction between the leucine residues and aromatic phenylalanine residues.

The results of the reduction in the hemolytic activity of BMAP-27 showed remarkable similarity with our previously reported results on the hemolytic activity of alanine-substituted analogues of melittin and LZP peptide (*26*, *27*). Besides the hemolytic activity, the cytotoxic activity of BMAP-27 and its analogues was checked against murine 3T3 cells by MTT assay, which also showed an appreciable decrease after the substitution of phenylalanine or leucine with alanine in the phenylalanine or leucine zipper sequence of BMAP-27, respectively. Collectively, the data indicated a general role of these heptad repeat sequences in maintaining the toxic activity of the antimicrobial peptides containing these sequence elements. One of the salient features of the BMAP-27 sequence is the presence of a phenylalanine zipper sequence. The results presented here demonstrate that the phenylalanine zipper sequence also plays a role similar to that of the leucine zipper sequence in the assembly of BMAP-27 on hRBCs. A previous study showed that 21-residue alanine, lysine, and phenylalanine rich peptides containing the phenylalanine zipper sequence self-assembled in an aqueous environment and exhibited toxicity against 3T3 cells (*44*). A magainin variant, MSI-78, containing a phenylalanine zipper was reported to form a dimer in DPC micelles by NMR study (*53*). However, permeabilization of mammalian cells and bacteria or assembly and localization of these peptides onto any of the cells have not been found, to the best of our knowledge.

In summary, considering the previous results, it appears that leucine or phenylalanine zipper sequence elements play a pre-

dominant role in maintaining the cytotoxic activity of BMAP-27 against mammalian cells. Thus, the presence of a leucine or phenylalanine zipper sequence or probably a heptad repeat in general provides a convenient way of incorporating a minor amino acid substitution in designing peptides with selective lytic activity against microorganisms.

ACKNOWLEDGMENT

We are extremely thankful to A. L. Vishwakarma for recoding the flow cytometry profiles. Manish Singh, Electron Microscopy Unit, CDRI, is acknowledged for assistance in recording the confocal microscopy images. J.K.G. dedicates this article to Prof. K. R. K. Easwaran, emeritus professor, Molecular Biophysics Unit, Indian Institute of Science, Bangalore with deep respect and gratitude.

SUPPORTING INFORMATION AVAILABLE

Antibacterial activity of BMAP-27 and its analogues against Gram-positive and Gram-negative bacteria was examined in the presence of serum (Table 1). The data show a varying degree of inhibition of bactericidal activity of the peptides by the plasma proteins present in the serum. Activity of labeled peptides was determined to check whether labeling of BMAP-27 and its analogues by fluorescent probes disturbed their functional property. Panels A−G of Figure 1 show that *E. coli* ATCC 10536 bound to NBD-labeled peptides were also stained by PI, which was comparable to the staining of bacteria by their unlabeled versions. Panel H shows that rhodamine labeling of BMAP-27 and its analogues did not have a significant effect on their bactericidal activities. The pore forming property of BMAP-27 and its analogues was determined by monitoring the peptide-induced release of calcein from calcein-entrapped zwitterionic (PC/Chol) and negatively charged (PC/PG) lipid vesicles (Figure 2). ANS binding of peptides indicated that BMAP-27 was more aggregated in an aqueous environment than its analogues (Figure 3). Self-assembly of BMAP-27 and its selected analogues on bacteria and hRBCs was examined by confocal microscopy studies with the help of photobleaching of acceptor molecules (Figure 4). BMAP-27 as well as its analogues self-assembled onto bacteria. However, BMAP-27 analogues did not bind or self-assemble appreciably on hRBCs. The amino acid sequence of a BMAP-27 analogue, which possesses the same amino acid composition as the parent molecule with an only minor amino acid modification in the zipper sequence, is shown Figure 5 along with its bactericidal, cytotoxic activities. Furthermore, the ability of this analogue (SCR-BMAP-27) to induce damage in the membrane organization of bacteria and mammalian cells was studied (Figure 5). This material is available free of charge via the Internet at http://pubs.acs.org.

REFERENCES

1. Boman, H. G. (1995) Peptide antibiotics and their role in innate immunity. *Annu. Rev. Immunol. 13*, 61–92.
2. Ramanathan, B., Davis, E. G., Ross, C. R., and Blecha, F. (2002) Cathelicidins: Microbicidal activity, mechanisms of action, and roles in innate immunity. *Microbes Infect. 4*, 361–372.
3. Lehrer, R. I., Lichtenstein, A. K., and Ganz, T. (1993) Defensins: Antimicrobial and cytotoxic peptides of mammalian cells. *Annu. Rev. Immunol. 11*, 105–128.
4. Hancock, R. E. (2001) Cationic peptides: Effectors in innate immunity and novel antimicrobials. *Lancet Infect. Dis. 1*, 156–164.
5. Risso, A. (2000) Leukocyte antimicrobial peptides: Multifunctional effector molecules of innate immunity. *J. Leukocyte Biol. 68*, 785–792.
6. Gennaro, R., and Zanetti, M. (2000) Structural features and biological activities of the cathelicidin-derived antimicrobial peptides. *Biopolymers 55*, 31–49.
7. Gennaro, R., Skerlavaj, B., and Romeo, D. (1989) Purification, composition, and activity of two bactenecins, antibacterial peptides of bovine neutrophils. *Infect. Immun. 57*, 3142–3146.
8. Bals, R., and Wilson, J. M. (2003) Cathelicidins: A family of multifunctional antimicrobial peptides. *Cell. Mol. Life Sci. 60*, 711–720.
9. Zanetti, M., Gennaro, R., and Romeo, D. (1995) Cathelicidins: A novel protein family with a common proregion and a variable C-terminal antimicrobial domain. *FEBS Lett. 374*, 1–5.
10. Travis, S. M., Anderson, N. N., Forsyth, W. R., Espiritu, C., Conway, B. D., Greenberg, E. P., McCray, P. B., Jr., Lehrer, R. I., Welsh, M. J., and Tack, B. F. (2000) Bactericidal activity of mammalian cathelicidin-derived peptides. *Infect. Immun. 68*, 2748–2755.
11. Lehrer, R. I., and Ganz, T. (2002) Cathelicidins: A family of endogenous antimicrobial peptides. *Curr. Opin. Hematol. 9*, 18–22.
12. Durr, U. H., Sudheendra, U. S., and Ramamoorthy, A. (2006) LL-37, the only human member of the cathelicidin family of antimicrobial peptides. *Biochim. Biophys. Acta 1758*, 1408–1425.
13. Zasloff, M. (2002) Antimicrobial peptides of multicellular organisms. *Nature 415*, 389–395.
14. Carretero, M., Escamez, M. J., Garcia, M., Duarte, B., Holguin, A., Retamosa, L., Jorcano, J. L., Rio, M. D., and Larcher, F. (2008) In vitro and in vivo wound healing-promoting activities of human cathelicidin LL-37. *J. Invest. Dermatol. 128*, 223–236.
15. Dorschner, R. A., Pestonjamasp, V. K., Tamakuwala, S., Ohtake, T., Rudisill, J., Nizet, V., Agerberth, B., Gudmundsson, G. H., and Gallo, R. L. (2001) Cutaneous injury induces the release of cathelicidin anti-microbial peptides active against group A *Streptococcus*. *J. Invest. Dermatol. 117*, 91–97.
16. Koczulla, R., von Degenfeld, G., Kupatt, C., Krotz, F., Zahler, S., Gloe, T., Issbrucker, K., Unterberger, P., Zaiou, M., Lebherz, C., Karl, A., Raake, P., Pfosser, A., Boekstegers, P., Welsch, U., Hiemstra, P. S., Vogelmeier, C., Gallo, R. L., Clauss, M., and Bals, R. (2003) An angiogenic role for the human peptide antibiotic LL-37/hCAP-18. *J. Clin. Invest. 111*, 1665–1672.
17. Lande, R., Gregorio, J., Facchinetti, V., Chatterjee, B., Wang, Y. H., Homey, B., Cao, W., Wang, Y. H., Su, B., Nestle, F. O., Zal, T., Mellman, I., Schroder, J. M., Liu, Y. J., and Gilliet, M. (2007) Plasmacytoid dendritic cells sense self-DNA coupled with antimicrobial peptide. *Nature 449*, 564–569.
18. Gudmundsson, G. H., Agerberth, B., Odeberg, J., Bergman, T., Olsson, B., and Salcedo, R. (1996) The human gene FALL39 and processing of the cathelin precursor to the antibacterial peptide LL-37 in granulocytes. *Eur. J. Biochem. 238*, 325–332.
19. Frohm, M., Agerberth, B., Ahangari, G., Stahle-Backdahl, M., Liden, S., Wigzell, H., and Gudmundsson, G. H. (1997) The expression of the gene coding for the antibacterial peptide LL-37 is induced in human keratinocytes during inflammatory disorders. *J. Biol. Chem. 272*, 15258–15263.
20. Johansson, J., Gudmundsson, G. H., Rottenberg, M. E., Berndt, K. D., and Agerberth, B. (1998) Conformation-dependent antibacterial activity of the naturally occurring human peptide LL-37. *J. Biol. Chem. 273*, 3718–3724.
21. Hancock, R. E., and Lehrer, R. (1998) Cationic peptides: A new source of antibiotics. *Trends Biotechnol. 16*, 82–88.
22. Zelezetsky, I., Pontillo, A., Puzzi, L., Antcheva, N., Segat, L., Pacor, S., Crovella, S., and Tossi, A. (2006) Evolution of the primate cathelicidin. Correlation between structural variations and antimicrobial activity. *J. Biol. Chem. 281*, 19861–19871.
23. Morgera, F., Vaccari, L., Antcheva, N., Scaini, D., Pacor, S., and Tossi, A. (2009) Primate cathelicidin orthologues display different structures and membrane interactions. *Biochem. J. 417*, 727–735.
24. Zanetti, M., Gennaro, R., and Romeo, D. (1997) The cathelicidin family of antimicrobial peptide precursors: A component of the oxygen-independent defense mechanisms of neutrophils. *Ann. N.Y. Acad. Sci. 832*, 147–162.
25. Skerlavaj, B., Gennaro, R., Bagella, L., Merluzzi, L., Risso, A., and Zanetti, M. (1996) Biological characterization of two novel cathelicidin-derived peptides and identification of structural requirements for their antimicrobial and cell lytic activities. *J. Biol. Chem. 271*, 28375–28381.
26. Asthana, N., Yadav, S. P., and Ghosh, J. K. (2004) Dissection of antibacterial and toxic activity of melittin: A leucine zipper motif plays a crucial role in determining its hemolytic activity but not antibacterial activity. *J. Biol. Chem. 279*, 55042–55050.
27. Ahmad, A., Yadav, S. P., Asthana, N., Mitra, K., Srivastava, S. P., and Ghosh, J. K. (2006) Utilization of an amphipathic leucine zipper

sequence to design antibacterial peptides with simultaneous modulation of toxic activity against human red blood cells. *J. Biol. Chem. 281*, 22029–22038.
28. Fields, G. B., and Noble, R. L. (1990) Solid phase peptide synthesis utilizing 9-fluorenylmethoxycarbonyl amino acids. *Int. J. Pept. Protein Res. 35*, 161–214.
29. Yadav, S. P., Kundu, B., and Ghosh, J. K. (2003) Identification and characterization of an amphipathic leucine zipper-like motif in *Escherichia coli* toxin hemolysin E. Plausible role in the assembly and membrane destabilization. *J. Biol. Chem. 278*, 51023–51034.
30. Oren, Z., and Shai, Y. (1997) Selective lysis of bacteria but not mammalian cells by diastereomers of melittin: Structure-function study. *Biochemistry 36*, 1826–1835.
31. Sal-Man, N., Oren, Z., and Shai, Y. (2002) Preassembly of membrane-active peptides is an important factor in their selectivity toward target cells. *Biochemistry 41*, 11921–11930.
32. Mangoni, M. L., Maisetta, G., Di Luca, M., Gaddi, L. M., Esin, S., Florio, W., Brancatisano, F. L., Barra, D., Campa, M., and Batoni, G. (2008) Comparative analysis of the bactericidal activities of amphibian peptide analogues against multidrug-resistant nosocomial bacterial strains. *Antimicrob. Agents Chemother. 52*, 85–91.
33. Nordahl, E. A., Rydengard, V., Morgelin, M., and Schmidtchen, A. (2005) Domain 5 of high molecular weight kininogen is antibacterial. *J. Biol. Chem. 280*, 34832–34839.
34. Papo, N., Braunstein, A., Eshhar, Z., and Shai, Y. (2004) Suppression of human prostate tumor growth in mice by a cytolytic D-,L-amino Acid Peptide: Membrane lysis, increased necrosis, and inhibition of prostate-specific antigen secretion. *Cancer Res. 64*, 5779–5786.
35. Yadav, S. P., Ahmad, A., Pandey, B. K., Verma, R., and Ghosh, J. K. (2008) Inhibition of lytic activity of *Escherichia coli* toxin hemolysin E against human red blood cells by a leucine zipper peptide and understanding the underlying mechanism. *Biochemistry 47*, 2134–2142.
36. Sims, P. J., Waggoner, A. S., Wang, C. H., and Hoffman, J. F. (1974) Studies on the mechanism by which cyanine dyes measure membrane potential in red blood cells and phosphatidylcholine vesicles. *Biochemistry 13*, 3315–3330.
37. Loew, L. M., Rosenberg, I., Bridge, M., and Gitler, C. (1983) Diffusion potential cascade. Convenient detection of transferable membrane pores. *Biochemistry 22*, 837–844.
38. Zhang, L., Rozek, A., and Hancock, R. E. (2001) Interaction of cationic antimicrobial peptides with model membranes. *J. Biol. Chem. 276*, 35714–35722.
39. Pan, Y. L., Cheng, J. T., Hale, J., Pan, J., Hancock, R. E., and Straus, S. K. (2007) Characterization of the structure and membrane interaction of the antimicrobial peptides aurein 2.2 and 2.3 from Australian southern bell frogs. *Biophys. J. 92*, 2854–2864.
40. Hawrani, A., Howe, R. A., Walsh, T. R., and Dempsey, C. E. (2008) Origin of low mammalian cell toxicity in a class of highly active antimicrobial amphipathic helical peptides. *J. Biol. Chem. 283*, 18636–18645.
41. Allen, T. M., and Cleland, L. G. (1980) Serum-induced leakage of liposome contents. *Biochim. Biophys. Acta 597*, 418–426.
42. Greenfield, N., and Fasman, G. D. (1969) Computed circular dichroism spectra for the evaluation of protein conformation. *Biochemistry 8*, 4108–4116.
43. Wu, C. S., Ikeda, K., and Yang, J. T. (1981) Ordered conformation of polypeptides and proteins in acidic dodecyl sulfate solution. *Biochemistry 20*, 566–570.
44. Javadpour, M. M., and Barkley, M. D. (1997) Self-assembly of designed antimicrobial peptides in solution and micelles. *Biochemistry 36*, 9540–9549.
45. Giddings, K. S., Johnson, A. E., and Tweten, R. K. (2003) Redefining cholesterol's role in the mechanism of the cholesterol-dependent cytolysins. *Proc. Natl. Acad. Sci. U.S.A. 100*, 11315–11320.
46. Sekar, R. B., and Periasamy, A. (2003) Fluorescence resonance energy transfer (FRET) microscopy imaging of live cell protein localizations. *J. Cell Biol. 160*, 629–633.
47. Chigaev, A., Buranda, T., Dwyer, D. C., Prossnitz, E. R., and Sklar, L. A. (2003) FRET detection of cellular α4-integrin conformational activation. *Biophys. J. 85*, 3951–3962.
48. Wouters, F. S., and Bastiaens, P. I. (2001) Imaging protein-protein interactions by fluorescence resonance energy transfer (FRET) microscopy. Current Protocols in Protein Science , Chapter 19, Unit 19, p 5, Wiley, New York.
49. Van Munster, E. B., Kremers, G. J., Adjobo-Hermans, M. J., and Gadella, T. W., Jr. (2005) Fluorescence resonance energy transfer (FRET) measurement by gradual acceptor photobleaching. *J. Microsc. 218*, 253–262.
50. Dhe-Paganon, S., Werner, E. D., Nishi, M., Hansen, L., Chi, Y. I., and Shoelson, S. E. (2004) A phenylalanine zipper mediates APS dimerization. *Nat. Struct. Mol. Biol. 11*, 968–974.
51. Ciornei, C. D., Sigurdardottir, T., Schmidtchen, A., and Bodelsson, M. (2005) Antimicrobial and chemoattractant activity, lipopolysaccharide neutralization, cytotoxicity, and inhibition by serum of analogs of human cathelicidin LL-37. *Antimicrob. Agents Chemother. 49*, 2845–2850.
52. Oren, Z., Lerman, J. C., Gudmundsson, G. H., Agerberth, B., and Shai, Y. (1999) Structure and organization of the human antimicrobial peptide LL-37 in phospholipid membranes: Relevance to the molecular basis for its non-cell-selective activity. *Biochem. J. 341* (Part 3), 501–513.
53. Porcelli, F., Buck-Koehntop, B. A., Thennarasu, S., Ramamoorthy, A., and Veglia, G. (2006) Structures of the dimeric and monomeric variants of magainin antimicrobial peptides (MSI-78 and MSI-594) in micelles and bilayers, determined by NMR spectroscopy. *Biochemistry 45*, 5793–5799.